The University of Sydney

Department of Civil Engineering
Sydney NSW 2006
AUSTRALIA

http://www.civil.usyd.edu.au/

Centre for Advanced Structural Engineering

Bifurcation of Locally Buckled Channel Columns

Research Report No R760

Ben Young BSc BE
Kim JR Rasmussen MScEng PhD

1997

Copyright Notice

Department of Civil Engineering, Research Report R760
Bifurcation of Locally Buckled Channel Columns

B.Young@civil.usyd.edu.au, K.Rasmussen@civil.usyd.edu.au

Published by:
Department of Civil Engineering
The University of Sydney
Sydney NSW 2006
AUSTRALIA

1997

http://www.civil.usyd.edu.au

BIFURCATION OF LOCALLY BUCKLED CHANNEL COLUMNS

B. Young, B.Sc., B.E.
and
K.J.R. Rasmussen, M.Sc.Eng., Ph.D.

Department of Civil Engineering, University of Sydney,
NSW 2006, Australia

Abstract

The report derives the governing equations for the fundamental and bifurcated states of members with singly symmetric cross-sections that locally buckle in the fundamental state. The members are subject to pure compression and assumed to be geometrically perfect in the overall sense. The method of analysis uses elastic and inelastic geometric nonlinear finite strip buckling analyses to determine the tangent rigidities of the locally buckled section. These rigidities are substituted into the equations for overall flexural and flexural-torsional buckling to obtain the bifurcation loads. The effect of yielding is highlighted through a parametric study. The overall bifurcation loads are compared with a series of tests of fixed-ended plain channel columns. The variation of the bifurcation loads with the length is shown to be in good agreement with the tests. The bifurcation loads are shown to be sensitive to the magnitudes of local and overall geometric imperfections.

TABLE OF CONTENTS

APPENDIX

1 INTRODUCTION

The behaviour of thin-walled singly symmetric columns is greatly influenced by the support conditions. It is possible to gain knowledge of the behaviour of thin-walled singly symmetric members that undergo local buckling prior to overall failure by establishing the governing equations for the fundamental and bifurcated states. By using the governing equations for the fundamental state, the different behaviour of locally buckled pin-ended and fixed-ended singly symmetric columns can be demonstrated. It can be shown that fixed-ended singly symmetric columns exhibit overall bifurcation behaviour in the case of vanishing overall geometric imperfections, while pin-ended singly symmetric columns do not. The bifurcation equations are established and applied to plain channel sections in this report.

The primary effect of local buckling is to reduce the member stiffnesses against overall flexure and torsion. Consequently, bifurcation in an overall mode can be calculated by using the stiffness of the locally buckled cross-section rather than the stiffness of the undistorted cross-section. This result has been used widely (Bijlaard and Fisher, 1953 and Hancock, 1981) to determine the flexural buckling load of locally buckled doubly symmetric columns. In this case, the buckling load can be obtained simply by replacing the flexural rigidity (EI) of the unbuckled section by the flexural rigidity of the locally buckled section in the Euler formula.

The flexural-torsional buckling can be analysed using a similar approach, in which case the stiffnesses of the locally buckled member against flexure and torsion are required. Bradford and Hancock (1984) analysed the bifurcation of locally buckled beams by employing a nonlinear finite strip method to determine the flexural rigidity of the section in minor axis bending. The minor axis rigidity was also used for determining approximately the warping rigidity of the locally buckled section. The method was applied to doubly symmetric I-sections in uniform bending.

In Rasmussen (1995), the bifurcation analysis of locally buckled members was formally described by deriving the governing equations for the fundamental and bifurcated states. The analysis was applicable to members of arbitrary cross-section shapes subjected to arbitrary types of loading. The members were assumed to be geometrically perfect in the overall sense

but could include imperfections in the local mode. The bifurcation analysis described in Rasmussen (1995) is applied in the present report to singly symmetric columns, for which the tangent rigidities of a locally buckled section are obtained by using elastic and inelastic nonlinear finite strip methods. The tangent rigidities are substituted into the flexural and flexural-torsional equations for the overall bifurcation loads. The bifurcation loads are compared with tests of fixed-ended plain channel columns. The effect of yielding is highlighted through a parametric study and by comparing the elastic and inelastic bifurcation loads.

2 BIFURCATION OF LOCALLY BUCKLED SINGLY SYMMETRIC COLUMNS

2.1 Model of the Locally Buckled Member

The analysis described in this section applies to cross-sections composed of thin plates. The component plates are assumed to buckle *locally* before overall buckling such that plate deflections at junctions are negligible, as shown in Fig. 1 for a plain channel in compression. Figure 2 shows the local buckling modes of other typical singly symmetric cross-sections in compression.

By recognising that the effect of local buckling on the overall behaviour is to reduce the stiffness of the member, a simple model follows by assuming that the locally buckled cross-section consists of an assembly of narrow strips, whose tangential stiffnesses (E_t) vary around the cross-section as functions of the extent of local buckling. This simple model allows the effect of local buckling, which causes a *geometrical* loss of stiffness, to be considered as a *material* effect in the overall bifurcation analysis, in so far as the effect is to change the initial stiffness (E). Consequently, it allows the formulation of bifurcation of thin-walled members with an undistorted cross-section to be used by changing only the stress-strain relations, as described in Rasmussen (1995).

2.2 Governing Equations for the Fundamental and Bifurcated States

The governing equations can be expressed in terms of the generalised displacements (u, v, w, ϕ) which are assumed to refer to the shear centre of the undistorted cross-section. The derivation applies to general types of cross-section. It is based on an assumption of small fundamental state displacements and uses a set of tangent rigidities, defined as,

$$(EA)_t = \int_A E_t^{w'}\, dA \tag{1}$$

$$(ES_x)_t = \int_A E_t^{w'} y\, dA = \int_A E_t^{v''} y\, dA \tag{2}$$

$$(ES_y)_t = \int_A E_t^{w'} x\, dA = \int_A E_t^{u''} x\, dA \tag{3}$$

$$(ES_\omega)_t = \int_A E_t^{w'} \omega\, dA = \int_A E_t^{\phi''} \omega\, dA \tag{4}$$

$$(EI_x)_t = \int_A E_t^{v''} y^2\, dA \tag{5}$$

$$(EI_y)_t = \int_A E_t^{u''} x^2\, dA \tag{6}$$

$$(EI_\omega)_t = \int_A E_t^{\phi''} \omega^2\, dA \tag{7}$$

$$(EI_{xy})_t = \int_A E_t^{v''} xy\, dA = \int_A E_t^{u''} xy\, dA \tag{8}$$

$$(EI_{x\omega})_t = \int_A E_t^{\phi''} y\omega\, dA = \int_A E_t^{v''} y\omega\, dA \tag{9}$$

$$(EI_{y\omega})_t = \int_A E_t^{\phi''} x\omega\, dA = \int_A E_t^{u''} x\omega\, dA \tag{10}$$

$$(GJ)_t = \int_A G_t 4n^2\, dA \tag{11}$$

in which the tangent shear modulus (G_t) may be assumed equal to the full shear modulus (G), and $E_t^{w'}$, $E_t^{u''}$, $E_t^{v''}$, $E_t^{\phi''}$ are the stiffnesses against axial straining (w'), bending in the (x, z)-plane (u''), bending in the (y, z)-plane (v'') and twisting (ϕ'') respectively, such that the incremental longitudinal stress is given by,

$$\dot{\sigma} = E_t^{w'}\dot{w}' + E_t^{u''}x(-\dot{u}'') + E_t^{v''}y(-\dot{v}'') + E_t^{\phi''}\omega(-\dot{\phi}'') \tag{12}$$

The general variational equation of incremental equilibrium of the fundamental state is given by (Rasmussen 1995),

$$\int_L \begin{Bmatrix} \dot{w}_o' \\ -\dot{u}_o'' \\ -\dot{v}_o'' \\ -\dot{\phi}_o'' \\ -\dot{\phi}_o' \end{Bmatrix}^T \begin{bmatrix} (EA)_t & (ES_y)_t & (ES_x)_t & (ES_\omega)_t & 0 \\ (ES_y)_t & (EI_y)_t & (EI_{xy})_t & (EI_{y\omega})_t & 0 \\ (ES_x)_t & (EI_{xy})_t & (EI_x)_t & (EI_{x\omega})_t & 0 \\ (ES_\omega)_t & (EI_{y\omega})_t & (EI_{x\omega})_t & (EI_\omega)_t & 0 \\ 0 & 0 & 0 & 0 & (GJ)_t \end{bmatrix} \begin{Bmatrix} \delta w' \\ -\delta u'' \\ -\delta v'' \\ -\delta\phi'' \\ -\delta\phi' \end{Bmatrix} dz$$

$$-\dot{\lambda}\left[\overline{N}\delta w + \overline{M}_y\delta u' + \overline{M}_x(-\delta v') + \overline{B}(-\delta\phi')\right]_{0,L} = 0 \tag{13}$$

where $\delta(\ )$ denotes a virtual quantity, $\dot{w}_o, \dot{u}_o, \dot{v}_o, \dot{\phi}_o$ are increments of fundamental state displacements, $\overline{N}, \overline{M}_x, \overline{M}_y, \overline{B}$ are applied reference stress resultants, defined by,

$$\overline{N} = \int_A q_z \, dA \tag{14}$$

$$\overline{M}_y = -\int_A q_z x \, dA \tag{15}$$

$$\overline{M}_x = \int_A q_z y \, dA \tag{16}$$

$$\overline{B} = \int_A q_z \omega \, dA \tag{17}$$

in which q_z is a longitudinal reference stress applied at the ends, and $\dot{\lambda}$ is the incremental load factor such that the total applied stress resultants are $\lambda\overline{N}, \lambda\overline{M}_x, \lambda\overline{M}_y$ and $\lambda\overline{B}$.

The incremental stress resultants of the fundamental state are defined as,

$$\dot{N}_o = \int_A \dot{\sigma}_o \, dA \tag{18}$$

$$\dot{M}_{xo} = \int_A \dot{\sigma}_o y \, dA \tag{19}$$

$$\dot{M}_{yo} = -\int_A \dot{\sigma}_o x \, dA \tag{20}$$

$$\dot{W}_o = \int_A \dot{\sigma}_o (x^2 + y^2) \, dA \tag{21}$$

where $\dot{\sigma}_o$ is the incremental longitudinal fundamental state stress.

The general variational equation of bifurcation is given by (Rasmussen 1995),

$$\int_L \begin{Bmatrix} w_b' \\ -u_b'' \\ -v_b'' \\ -\phi_b'' \\ -\phi_b' \end{Bmatrix}^T \begin{bmatrix} (EA)_t & (ES_y)_t & (ES_x)_t & (ES_\omega)_t & 0 \\ (ES_y)_t & (EI_y)_t & (EI_{xy})_t & (EI_{y\omega})_t & 0 \\ (ES_x)_t & (EI_{xy})_t & (EI_x)_t & (EI_{x\omega})_t & 0 \\ (ES_\omega)_t & (EI_{y\omega})_t & (EI_{x\omega})_t & (EI_\omega)_t & 0 \\ 0 & 0 & 0 & 0 & (GJ)_t \end{bmatrix} \begin{Bmatrix} \delta w' \\ -\delta u'' \\ -\delta v'' \\ -\delta\phi'' \\ -\delta\phi' \end{Bmatrix} dz$$

$$+\int_L \begin{Bmatrix} u_b' \\ u_b'' \\ v_b' \\ v_b'' \\ \phi_b \\ \phi_b' \end{Bmatrix}^T \begin{bmatrix} N_o & 0 & 0 & 0 & 0 & y_S N_o \\ 0 & 0 & 0 & 0 & M_{xo} & 0 \\ 0 & 0 & N_o & 0 & 0 & -x_S N_o \\ 0 & 0 & 0 & 0 & M_{yo} & 0 \\ 0 & M_{xo} & 0 & M_{yo} & 0 & 0 \\ y_S N_o & 0 & -x_S N_o & 0 & 0 & \begin{matrix}(x_S^2 + y_S^2)N_o + W_o \\ +2x_S M_{yo} - 2y_S M_{xo}\end{matrix} \end{bmatrix} \begin{Bmatrix} \delta u' \\ \delta u'' \\ \delta v' \\ \delta v'' \\ \delta\phi \\ \delta\phi' \end{Bmatrix} dz$$

$$-\left[\lambda_c \overline{M}_y (\phi_b \delta v' + v_b' \delta\phi) + \lambda_c \overline{M}_x (\phi_b \delta u' + u_b' \delta\phi)\right]_{0,L} = 0 \tag{22}$$

where w_b, u_b, v_b, ϕ_b are the buckling displacements, N_o, M_{xo}, M_{yo}, W_o are the fundamental state stress resultants, (x_S, y_S) are the shear centre coordinates, and λ_c is the critical load factor.

2.3 Singly Symmetric Cross-Section in Compression

2.3.1 Fundamental state

The (x, y)-axes of the singly symmetric cross-section are assumed to be principal and the x-axis is assumed to be the axis of symmetry. The sectorial coordinate (ω) is assumed to be normalised and refer to the shear centre. It then follows that ω is an odd function of y,

$$\omega(x, -y) = -\omega(x, y) \tag{23}$$

Since the local buckling deformations of a singly symmetric cross-section in compression are symmetric in magnitude about the symmetry axis, the tangent moduli ($E_t^{w'}$, $E_t^{u''}$, $E_t^{v''}$, $E_t^{\phi''}$) are even functions of y, and they satisfy

$$E_t(x, -y) = E_t(x, y) \tag{24}$$

Using eqns (23-24), it follows from eqns (2, 4, 8, 10) that

$$(ES_x)_t = (ES_\omega)_t = (EI_{xy})_t = (EI_{y\omega})_t = 0 \tag{25}$$

so that the incremental equilibrium equation (13) becomes,

$$\int_L \begin{Bmatrix} \dot{w}_o' \\ -\dot{u}_o'' \\ -\dot{v}_o'' \\ -\dot{\phi}_o'' \\ -\dot{\phi}_o' \end{Bmatrix}^T \begin{bmatrix} (EA)_t & (ES_y)_t & 0 & 0 & 0 \\ (ES_y)_t & (EI_y)_t & 0 & 0 & 0 \\ 0 & 0 & (EI_x)_t & (EI_{x\omega})_t & 0 \\ 0 & 0 & (EI_{x\omega})_t & (EI_\omega)_t & 0 \\ 0 & 0 & 0 & 0 & (GJ)_t \end{bmatrix} \begin{Bmatrix} \delta w' \\ -\delta u'' \\ -\delta v'' \\ -\delta\phi'' \\ -\delta\phi' \end{Bmatrix} dz$$

$$-\dot{\lambda}\left[\overline{N}\delta w + \overline{M}_y \delta u' + \overline{M}_x(-\delta v') + \overline{B}(-\delta\phi')\right]_{0,L} = 0 \tag{26}$$

By expanding and integrating this equation by parts the following differential equations and boundary conditions are obtained,

Differential equations:

$$((EA)_t \dot{w}_o')' - ((ES_y)_t \dot{u}_o'')' = 0 \tag{27}$$

$$-((ES_y)_t \dot{w}_o')'' + ((EI_y)_t \dot{u}_o'')'' = 0 \tag{28}$$

$$((EI_x)_t \dot{v}_o'')'' + ((EI_{x\omega})_t \dot{\phi}_o'')'' = 0 \tag{29}$$

$$((EI_{x\omega})_t \dot{v}_o'')'' + ((EI_\omega)_t \dot{\phi}_o'')'' - ((GJ)_t \dot{\phi}_o')' = 0 \tag{30}$$

Boundary conditions:

The boundary conditions are listed in Table 1 as derived from the variational equation (26). In the table, the upper and lower of stacked signs ($\pm$ or $\mp$) refer to $z = 0$ and $z = L$ respectively.

Geometric quantity restrained	or	Geometric quantity unrestrained	Eqn.
$\dot{w}_o = 0$		$(EA)_t \dot{w}_o' - (ES_y)_t \dot{u}_o'' \pm \dot{\lambda}\overline{N} = 0$	(31)
$\dot{u}_o = 0$		$((ES_y)_t \dot{w}_o')' - ((EI_y)_t \dot{u}_o'')' = 0$	(32)
$\dot{u}_o' = 0$		$-(ES_y)_t \dot{w}_o' + (EI_y)_t \dot{u}_o'' \pm \dot{\lambda}\overline{M}_y = 0$	(33)
$\dot{v}_o = 0$		$((EI_x)_t \dot{v}_o'')' + ((EI_{x\omega})_t \dot{\phi}_o'')' = 0$	(34)
$\dot{v}_o' = 0$		$(EI_x)_t \dot{v}_o'' + (EI_{x\omega})_t \dot{\phi}_o'' \mp \dot{\lambda}\overline{M}_x = 0$	(35)
$\dot{\phi}_o = 0$		$-((EI_{x\omega})_t \dot{v}_o'')' - ((EI_\omega)_t \dot{\phi}_o'')' + (GJ)_t \dot{\phi}_o' = 0$	(36)
$\dot{\phi}_o' = 0$		$(EI_{x\omega})_t \dot{v}_o'' + (EI_\omega)_t \dot{\phi}_o'' \mp \dot{\lambda}\overline{B} = 0$	(37)

$\pm, \mp$ upper sign refers to $z = 0$, lower to $z = L$

Table 1. Columns with singly symmetric thin-walled cross-sections

(Boundary conditions for fundamental state)

Simply supported columns

The boundary conditions for simply supported columns are shown in Fig. 3. Combined with Table 1, they provide the boundary conditions for the fundamental state. It follows from eqns (27-37) that w_o and u_o are coupled and that v_o and ϕ_o are coupled while there is no coupling between (w_o, u_o) and (v_o, ϕ_o).

By integrating eqns (27-30) and using eqns (31, 33, 35, 37), the following differential equations are obtained,

$$\left((EA)_t - \frac{(ES_y)_t^2}{(EI_y)_t}\right)\dot{w}_o' = -\dot{\lambda}\overline{N} \tag{38}$$

$$\left((EI_y)_t - \frac{(ES_y)_t^2}{(EA)_t}\right)\dot{u}_o'' = -\dot{\lambda}\overline{N}\frac{(ES_y)_t}{(EA)_t} \tag{39}$$

$$(EI_x)_t\dot{v}_o'' + (EI_{x\omega})_t\dot{\phi}_o'' = 0 \tag{40}$$

$$\left((EI_\omega)_t - \frac{(EI_{x\omega})_t^2}{(EI_x)_t}\right)\dot{\phi}_o'' - (GJ)_t\dot{\phi}_o = 0 \tag{41}$$

As discussed below, the tangent rigidities may be assumed to be constant along the length. Equations (38-41) may then be solved in conjunction with eqns (31, 32, 34, 36, 37) to produce,

$$\dot{w}_o = -\frac{\dot{\lambda}\overline{N}L}{\left((EA)_t - \frac{(ES_y)_t^2}{(EI_y)_t}\right)}\frac{z}{L} \tag{42}$$

$$\dot{u}_o = \frac{1}{2}\frac{\dot{\lambda}\overline{N}L^2\frac{(ES_y)_t}{(EA)_t}}{\left((EI_y)_t - \frac{(ES_y)_t^2}{(EA)_t}\right)}\left(\frac{z}{L} - \left(\frac{z}{L}\right)^2\right) \tag{43}$$

$$\dot{v}_o = 0 \tag{44}$$

$$\dot{\phi}_o = 0 \tag{45}$$

It follows from eqn. (43) that the axial force ($\overline{N}$) induces minor axis displacements (u_o) and so the column will not remain straight in the fundamental state, even though it is loaded through the geometric centroid of the undistorted cross-section. This conclusion reiterates the well-known result by Rhodes and Harvey (1977), that simply supported columns with singly symmetric cross-section undergo bending as a result of local buckling.

Using eqns (1, 3, 12, 18-21, 38-41), which apply whether the tangent rigidities are constant or not, the following incremental stress resultants are obtained

$$\dot{N}_o = -\dot{\lambda}\overline{N} \tag{46}$$

$$\dot{M}_{yo} = 0 \tag{47}$$

$$\dot{M}_{xo} = 0 \tag{48}$$

$$\dot{W}_o = \int_A \dot{\sigma}_o (x^2 + y^2)\, dA \tag{49}$$

It follows that the stress resultants are,

$$N_o = -\lambda\overline{N} \tag{50}$$

$$M_{yo} = 0 \tag{51}$$

$$M_{xo} = 0 \tag{52}$$

$$W_o = -\lambda \overline{W} \tag{53}$$

where

$$\overline{W} = -\int_A \sigma_o (x^2 + y^2)\, dA / \lambda \tag{54}$$

According to eqn. (51), the moment M_{yo} is zero despite the shift in the effective centroid which causes deflections (u_o). This is a result of the fact that the displacements of the fundamental state are assumed to be small in the present formulation, and hence, second order effects are ignored. The assumption of small fundamental state displacements is equivalent to establishing the equilibrium equations in the *undeformed* position, as shown in Fig. 4. In this case, the moment (M_{yo}) is zero in the fundamental state by equilibrium. (In algebraic terms, the moment is zero because it is made up of two effects that counteract each other exactly. The moment arising from the shift in the effective centroid and the moment arising from curvature ($\dot{u}_o''$) about the *y*-axis.) In the real column, the presence of high axial forces will amplify the bending deflections induced by local buckling. Consequently, the behaviour is characterised by nonlinear beam-column behaviour rather than by bifurcation buckling. A method for analysing this type of behaviour is described in Davids and Hancock (1987) and Rasmussen and Hancock (1991).

Equations (42-45) were deduced on the assumption of constant tangent rigidities. The tangent rigidities are functions of the generalised strains ($w_o', u_o'', v_o'', \phi_o''$) and so these must be constant for the tangent rigidities to be constant. It is reasonable to assume that the generalised strains are constant in the present analysis, since it is based on small fundamental state displacements and considers loads applied at the ends only, such that the loading term ($\dot{\lambda}\overline{N}$) in eqns (38-39) is constant along the length.

Fixed-ended columns

The boundary conditions for fixed-ended columns are shown in Fig. 5. Combined with Table 1, they provide the boundary conditions for the fundamental state.

Equations (27-30) may be integrated to produce,

$$\left((EA)_t - \frac{(ES_y)_t^2}{(EI_y)_t}\right)\dot{w}_o' = -\dot{\lambda}\overline{N} + (C_1 z + C_2)\frac{(ES_y)_t}{(EI_y)_t} \tag{55}$$

$$\left((EI_y)_t - \frac{(ES_y)_t^2}{(EA)_t}\right)\dot{u}_o'' = -\dot{\lambda}\overline{N}\frac{(ES_y)_t}{(EA)_t} + C_1 z + C_2 \tag{56}$$

$$(EI_x)_t \dot{v}_o'' + (EI_{x\omega})_t \dot{\phi}_o'' = C_3 z + C_4 \tag{57}$$

$$(EI_{x\omega})_t \dot{v}_o'' + (EI_\omega)_t \dot{\phi}_o'' - (GJ)_t \dot{\phi}_o = C_5 z + C_6 \tag{58}$$

where eqn. (31) has been utilised and C_1, C_2, C_3, C_4, C_5 and C_6 are arbitrary constants.

As discussed below, the tangent rigidities can be assumed to be constant along the length. It then follows by integrating eqns (55-58) and using eqns (31-37) that the incremental fundamental state displacements are given by,

$$\dot{w}_o = -\frac{\dot{\lambda}\overline{N}L}{(EA)_t}\frac{z}{L} \tag{59}$$

$$\dot{u}_o = 0 \tag{60}$$

$$\dot{v}_o = 0 \tag{61}$$

$$\dot{\phi}_o = 0 \tag{62}$$

It follows from eqns (60-62) that the column remains straight and untwisted although locally buckled. As a result, locally buckled fixed-ended columns with singly symmetric cross-section exhibit overall bifurcation behaviour when overall geometric imperfections are vanishing. The fact that the column remains straight and untwisted in the fundamental state justifies the assumption of constant tangent rigidities.

Using eqns (1, 12, 18-21, 55-58), the following incremental stress resultants are obtained,

$$\dot{N}_o = -\dot{\lambda}\overline{N} \tag{63}$$

$$\dot{M}_{yo} = 0 \tag{64}$$

$$\dot{M}_{xo} = 0 \tag{65}$$

$$\dot{W}_o = \int_A \dot{\sigma}_o (x^2 + y^2)\, dA \tag{66}$$

It follows that the stress resultants are

$$N_o = -\lambda\overline{N} \tag{67}$$

$$M_{yo} = 0 \tag{68}$$

$$M_{xo} = 0 \tag{69}$$

$$W_o = -\lambda\overline{W} \tag{70}$$

where

$$\overline{W} = -\int_A \sigma_o (x^2 + y^2)\, dA / \lambda \tag{71}$$

2.3.2 Bifurcated state - Fixed-ended columns

By using eqn. (25) and the stress resultants given by eqns (67-71), the bifurcation equation (22) becomes,

$$\int_L \begin{Bmatrix} w_b' \\ -u_b'' \\ -v_b'' \\ -\phi_b'' \\ -\phi_b' \end{Bmatrix}^T \begin{bmatrix} (EA)_t & (ES_y)_t & 0 & 0 & 0 \\ (ES_y)_t & (EI_y)_t & 0 & 0 & 0 \\ 0 & 0 & (EI_x)_t & (EI_{x\omega})_t & 0 \\ 0 & 0 & (EI_{x\omega})_t & (EI_\omega)_t & 0 \\ 0 & 0 & 0 & 0 & (GJ)_t \end{bmatrix} \begin{Bmatrix} \delta w' \\ -\delta u'' \\ -\delta v'' \\ -\delta\phi'' \\ -\delta\phi' \end{Bmatrix} dz$$
$$+\lambda_c \int_L \begin{Bmatrix} u_b' \\ u_b'' \\ v_b' \\ v_b'' \\ \phi_b \\ \phi_b' \end{Bmatrix}^T \begin{bmatrix} -\overline{N} & 0 & 0 & 0 & 0 & 0 \\ 0 & 0 & 0 & 0 & 0 & 0 \\ 0 & 0 & -\overline{N} & 0 & 0 & x_S\overline{N} \\ 0 & 0 & 0 & 0 & 0 & 0 \\ 0 & 0 & 0 & 0 & 0 & 0 \\ 0 & 0 & x_S\overline{N} & 0 & 0 & -x_S^2\overline{N} - \overline{W} \end{bmatrix} \begin{Bmatrix} \delta u' \\ \delta u'' \\ \delta v' \\ \delta v'' \\ \delta\phi \\ \delta\phi' \end{Bmatrix} dz = 0 \tag{72}$$

By expanding and integrating this equation by parts, the following differential equations and boundary conditions are obtained,

<u>Differential equations:</u>

$$((EA)_t w_b')' - ((ES_y)_t u_b'')' = 0 \tag{73}$$

$$-((ES_y)_t w_b')'' + ((EI_y)_t u_b'')'' + (\lambda_c \overline{N} u_b')' = 0 \tag{74}$$

$$((EI_x)_t v_b'')'' + ((EI_{x\omega})_t \phi_b'')'' + (\lambda_c \overline{N} v_b')' - (\lambda_c \overline{N} x_S \phi_b')' = 0 \tag{75}$$

$$\begin{aligned} &((EI_{x\omega})_t v_b'')'' + ((EI_\omega)_t \phi_b'')'' - ((GJ)_t \phi_b')' \\ &\quad - (\lambda_c \overline{N} x_S v_b')' + ((\lambda_c \overline{N} x_S^2 + \lambda_c \overline{W})\phi_b')' = 0 \end{aligned} \tag{76}$$

Boundary conditions:

The boundary conditions are listed in Table 2 as derived from the variational equation (72).

Geometric quantity restrained	or	Geometric quantity unrestrained	Eqn.
$w_b = 0$		$(EA)_t w_b' - (ES_y)_t u_b'' = 0$	(77)
$u_b = 0$		$-((ES_y)_t w_b')' + ((EI_y)_t u_b'')' + \lambda_c \overline{N} u_b' = 0$	(78)
$u_b' = 0$		$-(ES_y)_t w_b' + (EI_y)_t u_b'' = 0$	(79)
$v_b = 0$		$((EI_x)_t v_b'')' + ((EI_{x\omega})_t \phi_b'')' + \lambda_c \overline{N} v_b' - \lambda_c \overline{N} x_S \phi_b' = 0$	(80)
$v_b' = 0$		$(EI_x)_t v_b'' + (EI_{x\omega})_t \phi_b'' = 0$	(81)
$\phi_b = 0$		$-((EI_{x\omega})_t v_b'')' - ((EI_\omega)_t \phi_b'')' + (GJ)_t \phi_b'$ $+\lambda_c \overline{N} x_S v_b' - \lambda_c \overline{N} x_S^2 \phi_b' - \lambda_c \overline{W} \phi_b' = 0$	(82)
$\phi_b' = 0$		$(EI_{x\omega})_t v_b'' + (EI_\omega)_t \phi_b'' = 0$	(83)

Table 2. Columns with singly symmetric thin-walled cross-sections

(Boundary conditions for bifurcated state)

Using the result that the tangent rigidities are constant along the length, the bifurcation equations (73-83) are satisfied by the functions,

$$w_b = C_w \sin\left(\frac{2\pi z}{L}\right) \tag{84}$$

$$u_b = C_u \left(1 - \cos\left(\frac{2\pi z}{L}\right)\right) \tag{85}$$

$$v_b = C_v \left(1 - \cos\left(\frac{2\pi z}{L}\right)\right) \tag{86}$$

$$\phi_b = C_\phi \left(1 - \cos\left(\frac{2\pi z}{L}\right)\right) \tag{87}$$

which may be substituted into eqns (73-76) to produce the following determinant-equation,

$$\begin{vmatrix} (EA)_t & -\left(\frac{2\pi}{L}\right)(ES_y)_t & 0 & 0 \\ -\left(\frac{2\pi}{L}\right)(ES_y)_t & \left(\frac{2\pi}{L}\right)^2(EI_y)_t - \lambda_c\overline{N} & 0 & 0 \\ 0 & 0 & \left(\frac{2\pi}{L}\right)^2(EI_x)_t - \lambda_c\overline{N} & \left(\frac{2\pi}{L}\right)^2(EI_{x\omega})_t + \lambda_c\overline{N}x_S \\ 0 & 0 & \left(\frac{2\pi}{L}\right)^2(EI_{x\omega})_t + \lambda_c\overline{N}x_S & \left(\frac{2\pi}{L}\right)^2(EI_\omega)_t + (GJ)_t \\ & & & -\lambda_c\overline{N}x_S^2 - \lambda_c\overline{W} \end{vmatrix} = 0 \tag{88}$$

in which the first two rows pertain to w_b and u_b while the last two rows pertain to v_b and ϕ_b so that flexural buckling in (w_b, u_b) is uncoupled from flexural-torsional buckling in (v_b,ϕ_b). The critical load factors for flexural buckling (λ_{c_u}) and flexural-torsional buckling ($\lambda_{c_{v\phi}}$) are obtained from,

$$\lambda_{c_u} = \frac{\left(\frac{2\pi}{L}\right)^2\left((EI_y)_t - \frac{(ES_y)_t^2}{(EA)_t}\right)}{\overline{N}} \tag{89}$$

$$\lambda_{c_{v\phi}} = \frac{-B \pm \sqrt{B^2 - 4AC}}{2A} \tag{90}$$

where

$$A = \frac{\overline{N}\overline{W}}{r_o^2 + x_S^2} \tag{91}$$

$$B = -\overline{N}\left(P_x\frac{\frac{\overline{W}}{\overline{N}} + x_S^2}{r_o^2 + x_S^2} + P_z + 2\left(\frac{2\pi}{L}\right)^2\frac{x_S}{r_o^2 + x_S^2}(EI_{x\omega})_t\right) \tag{92}$$

$$C = P_x P_z - \left(\frac{2\pi}{L}\right)^4 \frac{(EI_{x\omega})_t^2}{r_o^2 + x_S^2} \tag{93}$$

$$P_x = \left(\frac{2\pi}{L}\right)^2 (EI_x)_t \tag{94}$$

$$P_z = \frac{\left(\frac{2\pi}{L}\right)^2 (EI_\omega)_t + (GJ)_t}{r_o^2 + x_S^2} \tag{95}$$

$$r_o^2 = \frac{I_P}{A} = \frac{I_x + I_y}{A} = \frac{\int_A (x^2 + y^2)\, dA}{A} \tag{96}$$

Equations (89-96) reproduce the classical flexural and flexural-torsional buckling equations in the case of undistorted cross-sections, for which $(ES_y)_t = (EI_{x\omega})_t = 0$ and $\overline{W} = \overline{N} r_o^2$. In eqn. (89), the term $(ES_y)_t^2 / (EA)_t$ arises because an axial force develops in a locally buckled singly symmetric section when subjected to curvature (u'') about the *y*-axis. Thus the $((EI_y)_t - (ES_y)_t^2 / (EA)_t)$-term is the flexural rigidity determined at constant axial force. The fact that an axial force develops during bending about the *y*-axis also explains the presence of longitudinal displacements (w_b) in the buckling mode, as demonstrated by eqn. (84). These are the displacements required to maintain constant axial force during overall bifurcation.

In eqns (92-93), the $(EI_{x\omega})_t$ -term results from the fact that a bimoment (B) is induced when a locally buckled singly symmetric section undergoes bending about the *x*-axis, and a bending moment (M_x) is induced when the section undergoes twisting. The reason why a bimoment is introduced when a locally buckled singly symmetric section undergoes bending about the *x*-axis is explained in Fig. 6. Figure 6a shows the fundamental state local buckling deformations of a plain channel section. The section is assumed to undergo bending (v'') about the *x*-axis from this state. The deflections and stresses ($\Delta\sigma^{v''}$) that develop as a result of such bending are shown in Figs 6b and 6c respectively. The sectorial coordinate (ω) of the channel section

is shown in Fig. 6d. It follows from the figures that $\Delta B^{v''} = \int_A \Delta\sigma^{v''}\,\omega\,dA = -(EI_{x\omega})_t(\Delta\sigma^{v''}) \neq 0$, and so $(EI_{x\omega})_t \neq 0$. Fig. 6a also shows the stresses that would develop if the section was undistorted. In this case, the stress is proportional to *y* and hence the bimoment $(\Delta B^{v''})$ caused by bending about the *x*-axis is zero as a result of the orthogonality of the *y*- and ω-coordinates. Consequently, $(EI_{x\omega})_t$ is zero for the undistorted cross-section.

2.4 Tangent Rigidities

The tangent rigidities of the locally buckled member may be determined from a nonlinear postbuckling analysis of a length of section equal to the local buckle half-wavelength (*l*). The analysis produces rigidities that are average values for this length of section. As described in Rasmussen (1995), the tangent rigidities can be calculated as,

$$(EA)_t = \frac{\partial N}{\partial w'} \cong \frac{\Delta N}{\Delta w'} \tag{97}$$

$$(ES_y)_t = \frac{\partial N}{-\partial u''} \cong \frac{\Delta N}{-\Delta u''} \quad \text{or} \quad (ES_y)_t = \frac{-\partial M_y}{\partial w'} \cong \frac{-\Delta M_y}{\Delta w'} \tag{98}$$

$$(EI_x)_t = \frac{\partial M_x}{-\partial v''} \cong \frac{\Delta M_x}{-\Delta v''} \tag{99}$$

$$(EI_y)_t = \frac{\partial M_y}{\partial u''} \cong \frac{\Delta M_y}{\Delta u''} \tag{100}$$

$$(EI_\omega)_t = \frac{\partial B}{-\partial \phi''} \cong \frac{\Delta B}{-\Delta \phi''} \tag{101}$$

$$(EI_{x\omega})_t = \frac{\partial B}{-\partial v''} \cong \frac{\Delta B}{-\Delta v''} \quad \text{or} \quad (EI_{x\omega})_t = \frac{\partial M_x}{-\partial \phi''} \cong \frac{\Delta M_x}{-\Delta \phi''} \tag{102}$$

In the present report, the tangent rigidities are determined using both elastic and inelastic nonlinear buckling analyses of a local buckle, as described and applied in Hancock (1985) and Key and Hancock (1993) respectively. While performing the nonlinear analysis, increments of generalised strains $(\Delta w', \Delta u'', \Delta v'', \Delta\phi'')$ are imposed using a set of equal and opposite end displacements and rotations,

$$\Delta w' = \frac{\Delta w(l) - \Delta w(0)}{l} = 2\frac{\Delta w(l)}{l} \tag{103}$$

$$\Delta(-u'') = -\frac{\Delta u'(l) - \Delta u'(0)}{l} = -2\frac{\Delta u'(l)}{l} \tag{104}$$

$$\Delta(-v'') = -\frac{\Delta v'(l) - \Delta v'(0)}{l} = -2\frac{\Delta v'(l)}{l} \tag{105}$$

$$\Delta(-\phi'') = -\frac{\Delta\phi'(l) - \Delta\phi'(0)}{l} = -2\frac{\Delta\phi'(l)}{l} \tag{106}$$

The increment of longitudinal displacement of a point (P) to be applied at the end cross-section ($z = l$) is,

$$\Delta w_P(l) = \Delta w(l) - x\Delta u'(l) - y\Delta v'(l) - \omega\Delta\phi'(l) \tag{107}$$

where $\Delta w(l)$ is a uniform displacement, $\Delta u'(l)$ and $\Delta v'(l)$ are rotations about the y- and x-axis respectively, and $\Delta\phi'(l)$ is a twist. The incremental displacement $(\Delta w_P(l))$ is superimposed onto the current fundamental state end displacements $(w_{P_o}(l))$. Thus, at a given load level, the tangent rigidities can be obtained from eqns (97-102) by applying, in turn, increments of generalised strain $(\Delta w', \Delta u'', \Delta v'', \Delta\phi'')$, calculating the corresponding incremental end displacements using eqns (103-107), and for each increment, computing the increments in stress resultants $(\Delta N, \Delta M_x, \Delta M_y, \Delta B)$.

3 COMPARISON OF BIFURCATION ANALYSIS AND EXPERIMENTAL RESULTS

3.1 General

The bifurcation loads ($\lambda_{c_u}\overline{N}, \lambda_{c_{v\phi}}\overline{N}$) derived in Section 2.3 of this report are applied to fixed-ended plain channel columns. The loads are compared with tests performed by Young and Rasmussen (1995a). Two cross-sections are analysed as detailed in Fig. 7 and Table 3. The sections are labelled as P36 and P48 according to their nominal flange widths of 36mm and 48mm respectively. The cross-section dimensions shown in Table 3 are averages of measured test specimen dimensions, as described in Young and Rasmussen (1995a). The specimens were produced by brake-pressing, and consequently, the corner radii (r_i) and the residual stresses were small and could be assumed to be negligible. Local and overall geometric imperfections were measured prior to testing. The measurement indicated that the overall minor axis flexural imperfections at mid-length of the P36 specimens were uniformly of the order of L/1500 where L is the specimen length. The largest overall minor axis flexural imperfections at mid-length of the P48 specimens was L/2500, as measured in the longest specimen of length 3500mm. The overall imperfections of the remaining P48 specimens were generally less than L/4000. Thus, the overall imperfections of the P48 specimens were significantly smaller than those of the P36 specimens. The measured local imperfections showed that the out-of-straightness of the free edge of the flanges was of the order of the plate thickness for all specimens. However, the component of the imperfection in the shape of the local buckling mode would be somewhat less than that. The measured local and overall geometric imperfection profiles are detailed in Young and Rasmussen (1995a).

The cross-sections have been analysed using an elastic finite strip buckling analysis (Hancock, 1978). The results are given in Table 4, in which E is the measured value of Young's modulus, σ_l is the local buckling stress and l is the local buckle half-wavelength. The corner radii and the residual stresses were not modelled in the analysis.

The tangent rigidities were determined using the elastic nonlinear finite strip local buckling analysis described by Hancock (1985) as well as an inelastic nonlinear finite strip buckling analysis described by Key and Hancock (1993). In the analyses, a length of section equal to the local buckle half-wavelength was subjected to increasing values of axial compression and at each load level, small increments of generalised strain $(\Delta w', \Delta u'', \Delta v'', \Delta\phi'')$ were applied. This allowed the tangent rigidities $((EA)_t, (ES_y)_t, (EI_x)_t, (EI_y)_t, (EI_\omega)_t, (EI_{x\omega})_t)$ to be obtained at each load level, as detailed in Section 2.4 of this report. Subsequently, the bifurcation curves were obtained by expressing eqns (89-96) in terms of the lengths (L) to cause flexural and flexural-torsional buckling at a given load. This procedure allowed the bifurcation curves to be obtained without iteration.

3.2 Elastic Bifurcation

The elastic bifurcation curves are shown in Figs 8 and 9 for sections P36 and P48 respectively. The bifurcation loads ($\lambda_{c_u}\overline{N}, \lambda_{c_{v\phi}}\overline{N}$) are shown as N_{cr} on the vertical axis, nondimensionalised with respect to the elastic local buckling load ($N_l = A\sigma_l$). The figures include the flexural (F) and flexural-torsional (FT) bifurcation curves of both the locally buckled and undistorted cross-sections. The curves are shown in Figs 8a and 9a for a magnitude (w_o) of the local geometric imperfection (in the shape of the local buckling mode) of $w_o = 0.02t$ and in Figs 8b and 9b for a magnitude of the local geometric imperfection of $w_o = 0.2t$.

The test results for the P36 section shown in Fig. 8 are lower than the bifurcation curves for both values of local imperfection. The discrepancy is attributed to overall geometric imperfections. Furthermore, the stub column test (L = 280mm) and the tests performed at L = 1000mm and 1500mm are likely to have been influenced by yielding before reaching the ultimate load. It follows from Fig. 8b that for a local imperfection magnitude of $w_o = 0.2t$, the variation of the elastic bifurcation curves with the length follows closely that of the test strengths in the range $L \geq$ 1500mm. The overall buckling mode observed in the tests was a flexural mode in all cases. The critical bifurcation loads of the locally buckled section shown in Fig. 8b concur with this result. It is particularly interesting to note that the critical mode is the flexural mode at all lengths despite the fact that the critical mode of the undistorted cross-

section is the flexural-torsional mode at lengths less than 2600mm. This is explained by the different effects of local buckling on the stiffnesses against flexural and flexural-torsional buckling. Figure 10a shows the tangent rigidities ($(EI_y)_t$, $(EI_x)_t$, $(EI_\omega)_t$) as functions of the load (N / N_l) for the P36 section obtained from the elastic nonlinear finite strip analysis. The rigidity curves are shown for four values of local geometric imperfection, w_o / t = 0.01, 0.05, 0.1 and 0.2. It follows that the stiffness against minor axis flexure ($(EI_y)_t$) drops more rapidly than the stiffnesses against major axis flexure ($(EI_x)_t$) and warping torsion ($(EI_\omega)_t$) for this section. This causes flexural buckling to be more critical than flexural-torsional buckling at short and intermediate lengths.

The test results for the P48 section are compared with the bifurcation curves in Fig. 9. The bifurcation curves are greatly influenced by the magnitude of local geometric imperfection. For a magnitude of $w_o = 0.02t$, several test strengths are higher than the bifurcation loads, while for a magnitude of $w_o = 0.2t$, the test strengths are slightly lower than the bifurcation loads, except for the strength obtained at L = 3000mm. As for the P36 section, the variation of the bifurcation curves with the length is similar to that of the test strengths at intermediate and long lengths.

The overall failure modes observed in the tests of the P48 section specimens were flexural modes for all lengths less than 3000mm, and flexural-torsional modes for L = 3000mm and L = 3500mm. The flexural modes at lengths less than 3000mm were associated with significant cross-section distortion while the flexural-torsional modes at lengths L = 3000mm and L = 3500mm were not. These failure modes are in agreement with those implied by the elastic bifurcation curves shown in Fig. 9.

3.3 Inelastic Bifurcation

The flexural (F) and flexural-torsional (FT) inelastic bifurcation curves of locally buckled cross-sections are also shown in Figs 8 and 9 for sections P36 and P48 respectively. The measured stress-strain curve was modelled in the analysis using the Ramberg-Osgood expression (Ramberg and Osgood, 1943),

$$\varepsilon = \frac{\sigma}{E_o} + 0.002\left(\frac{\sigma}{\sigma_{0.2}}\right)^n \tag{108}$$

where ε is the strain, σ is the stress, $\sigma_{0.2}$ is 0.2% proof stress, E_o is the initial modulus of elasticity and n is a parameter that describes the shape of the curve. In the limit, $n \to \infty$, the Ramberg-Osgood expression represents elastic-perfectly plastic material behaviour. The measured stress-strain curves (Young and Rasmussen, 1995a) were used to determine E_o, and the proof stresses $\sigma_{0.01}$ and $\sigma_{0.2}$, as shown in Table 4. The parameter n could be obtained from $\sigma_{0.01}$ and $\sigma_{0.2}$ using $n = \ln(0.01/0.2) / \ln(\sigma_{0.01}/\sigma_{0.2})$. This expression provided the values of n = 8 and n = 6 for the sections P36 and P48 respectively.

The test results for the P36 section shown in Figs 8a and 8b for local imperfection magnitudes of $w_o = 0.02t$ and $w_o = 0.2t$ respectively are lower than the inelastic bifurcation curves. As mentioned previously, the discrepancy is attributed to overall geometric imperfections. However, at short to intermediate lengths, the inelastic bifurcation curves follow much more closely the test strengths than the elastic bifurcation curves. As for the elastic bifurcation, the flexural buckling mode observed in the tests was accurately predicted at all lengths.

In Fig. 10b, the inelastic tangent rigidities ($(EI_y)_t$, $(EI_x)_t$, $(EI_\omega)_t$) are shown as functions of the load (N / N_l) for the P36 section obtained using n = 8. The rigidities follow a similar trend to the elastic rigidity curves shown in Fig. 10a indicating that the stiffness against minor axis flexure ($(EI_y)_t$) drops more rapidly than the stiffnesses against major axis flexure ($(EI_x)_t$) and warping torsion ($(EI_\omega)_t$) for this section, and that yielding accentuates the drop.

The test results for the P48 section are compared with the inelastic bifurcation curves in Figs 9a and 9b for local imperfection magnitudes of $w_o = 0.02t$ and $w_o = 0.2t$ respectively. For the locally buckled section ($N_{cr} / N_l \geq 1$), the inelastic flexural bifurcation curve is always lower than the inelastic flexural-torsional curve for both values of local imperfection. The predicted buckling modes were in agreement with the buckling modes observed in the tests. As for the elastic bifurcation curves, the inelastic bifurcation curves are also greatly influenced by the magnitude of local geometric imperfection. Several of the test strengths are higher than the bifurcation loads for a magnitude of $w_o = 0.02t$, while the test strengths are lower than or equal

to the bifurcation loads for a magnitude of $w_o = 0.2t$, except for the strength obtained at L = 3000mm. The variation of the bifurcation curves with the length is in good agreement with that of the test strengths.

For the purpose of demonstrating the effect of yielding on the bifurcation curves, three different material stress-strain curves, defined by $n = 5$, $n = 25$ and $n \rightarrow \infty$, were used to produce bifurcation curves, as shown in Fig. 11 for section P36 for a local imperfection magnitude of $w_o = 0.02t$. The flexural bifurcation loads are shown as N_{cr} on the vertical axis, nondimensionalised with respect to the elastic local buckling load (N_l). The figure shows the flexural bifurcation curves of the undistorted, elastic distorted and inelastic distorted cross-sections. For the locally buckled section ($N_{cr} / N_l \geq 1$), the flexural bifurcation curve for $n = 5$ lies well below that for $n \rightarrow \infty$ at intermediate column lengths. The flexural bifurcation curve for $n = 25$ lies between those for $n = 5$ and $n \rightarrow \infty$ at intermediate column lengths. The flexural bifurcation curve for $n = 5$ follows most closely that of the test strengths, as should be expected since the value $n = 8$ deduced from the measured stress-strain curve is closest to $n = 5$. For n = 25 and $n \rightarrow \infty$, the bifurcation load approaches a limiting value of $N_{cr} / N_l \cong 1.7$ at $L \cong$ 1000mm, but this is not the case for $n = 5$. This apparent limiting load is simply a statement of the fact that an ultimate load was reached in the inelastic finite strip analysis for $n = 25$ and $n \rightarrow \infty$ but not for $n = 5$. For $n = 25$ and $n \rightarrow \infty$, the bifurcation loads corresponding to $L <$ 1000mm were obtained from the tangent rigidities determined in the post-ultimate range of the finite strip analysis. These loads do not have physical relevance, since for $L <$ 1000mm the strength is simply the limiting load $N_{cr} / N_l \cong 1.7$ (the stub column strength) which is not a bifurcation load.

The tangent rigidities ($(EI_y)_t$, $(EI_x)_t$, $(EI_\omega)_t$) are shown in Fig. 12 for $n = 5$, $n = 25$ and $n \rightarrow \infty$. It appears that the initial drop in the minor axis flexural and warping-torsion tangent rigidities is steeper the smaller the value of n, leading to lower bifurcation curves as evidenced in Fig. 11. The attainment of an ultimate load in the inelastic finite strip analysis for $n = 25$ and $n \rightarrow \infty$ is also apparent from Fig. 12.

4 CONCLUSIONS

The analysis of the fundamental and bifurcated states of locally buckled singly-symmetric columns have been described and applied to a channel section. It is shown by solving the governing equations for the fundamental state that local buckling induces bending in a pin-ended singly symmetric column but not in a fixed-ended singly symmetric column. Consequently, only fixed-ended singly symmetric columns exhibit bifurcation behaviour.

In addition, a technique for determining overall flexural and flexural-torsional bifurcation loads of locally buckled singly-symmetric columns has been presented and applied to channel sections. It uses elastic and inelastic nonlinear finite strip buckling analyses to determine the tangent rigidities of the locally buckled section. The tangent rigidities are substituted into the overall flexural and flexural-torsional bifurcation equations.

The bifurcation loads of two plain channel section columns are compared with test results. Good agreement is found between the test strengths and the bifurcation loads obtained using the inelastic buckling analysis. However, at short lengths, the test strengths were significantly lower than the elastic bifurcation loads because of yielding.

The test strengths were generally lower than the bifurcation loads as a result of overall geometric imperfections. However, in some cases, where the local geometric imperfections were assumed to be very small, the test strengths were higher than the bifurcation curves. The inelastic bifurcation loads for different material stress-strain curves were presented using different values of the parameter n of the Ramberg-Osgood expression.

It is shown that for plain channel sections, local buckling reduces the stiffness against flexural buckling more severely than the stiffnesses against flexural-torsional buckling. As a result, failure of the locally buckled section may be in a flexural mode even though the critical mode is a flexural-torsional mode according to classical theory of thin-walled members with undistorted cross-sections.

5 ACKNOWLEDGMENTS

The first author was supported by grants from the Australian Postgraduate Research Award Scheme, the Civil and Mining Engineering Foundation and the Centre for Advanced Structural Engineering of the University of Sydney.

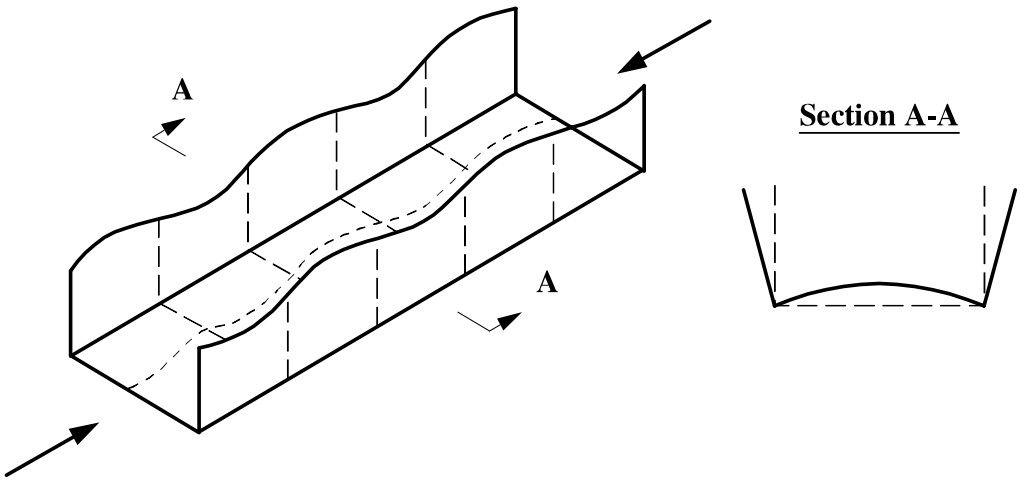

Fig. 1. Locally Buckled plain channel in compression

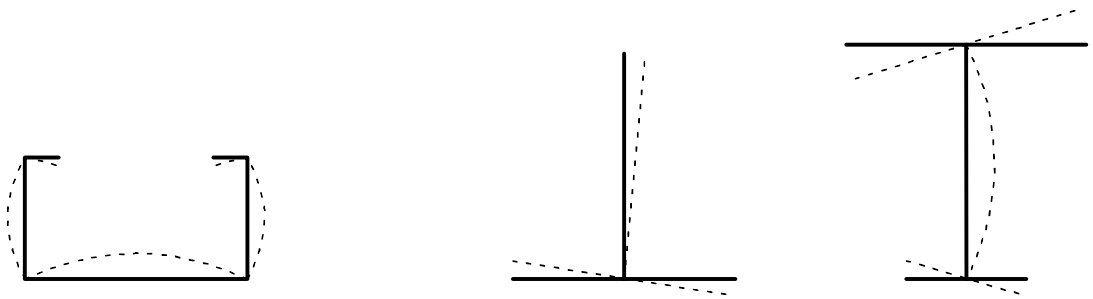

Fig. 2. Local buckling modes of typical singly symmetric cross-sections in compression

Fig. 3. Boundary conditions for simply supported columns

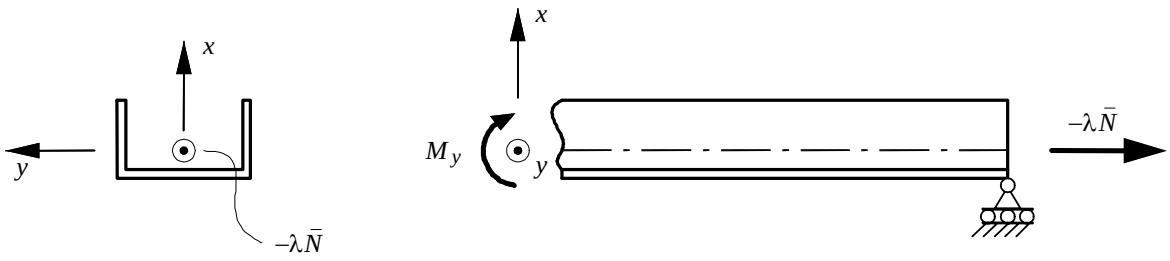

Fig. 4. Internal moment (M_y) in locally buckled singly symmetric column, (assuming small fundamental state displacements)

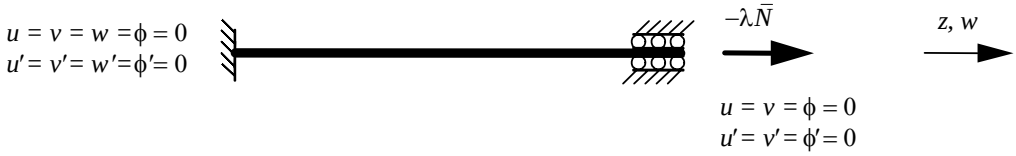

Fig. 5. Boundary conditions for fixed-ended columns

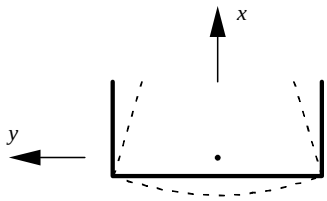

(a) Fundamental state local displacements

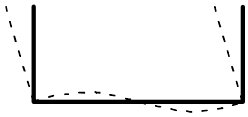

(b) Local displacement induced by $\Delta v''$

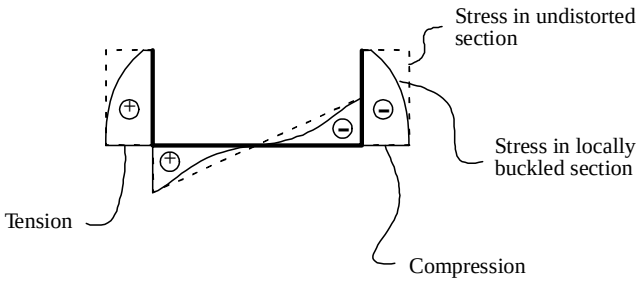

(c) Longitudinal stress $(\Delta\sigma^{v''})$ induced by $\Delta v''$

(d) Sectorial coordinate (ω)

Fig. 6. Bimoment in locally buckled singly symmetric section

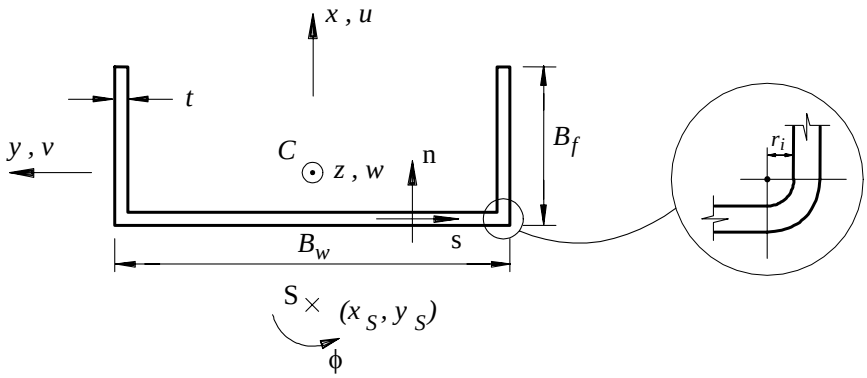

Fig. 7. Nomenclature for plain channel section

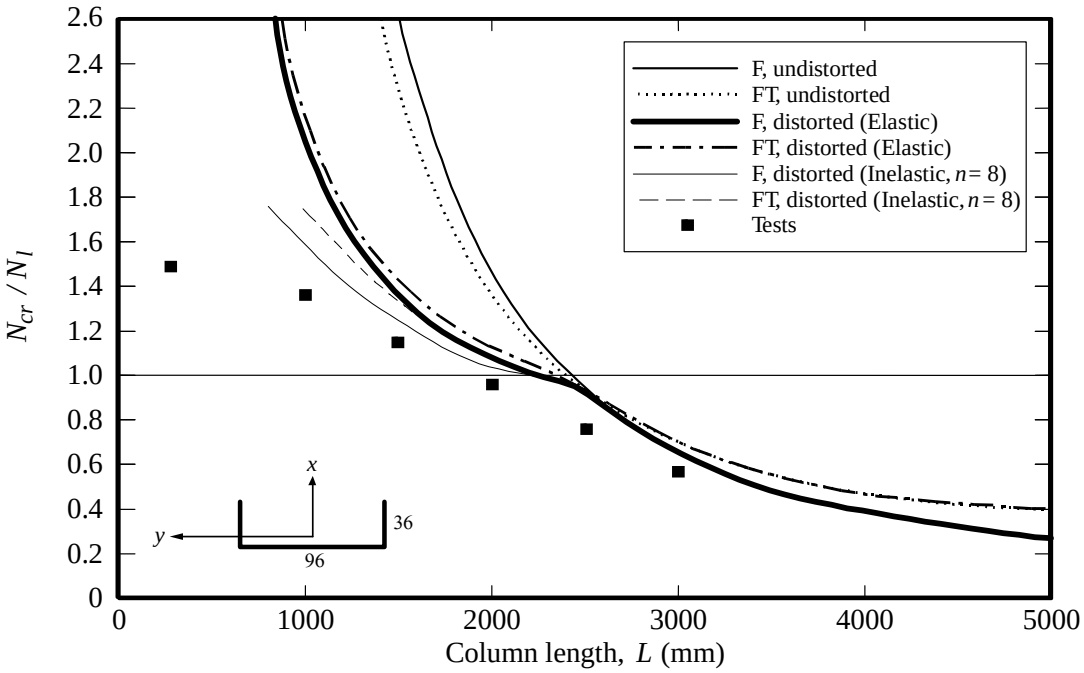

(a) w_o/t = 0.02

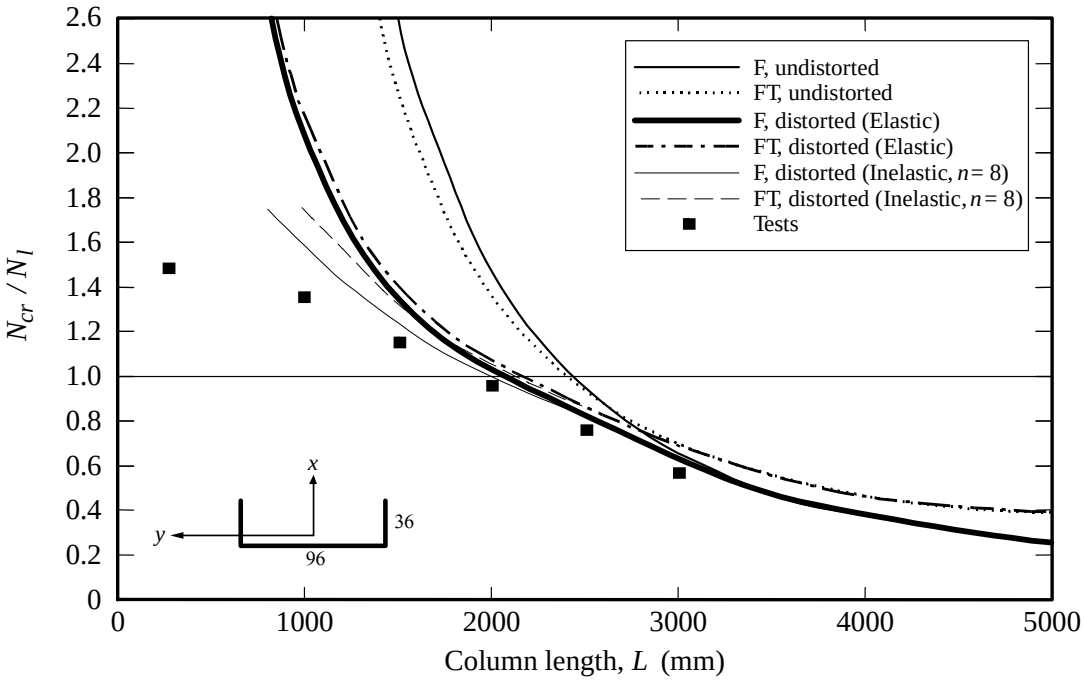

(b) w_o/t = 0.2

Fig. 8. Nondimensionalised load (N_{cr}/N_l) vs column length (L) for fixed-ended P36 channel section

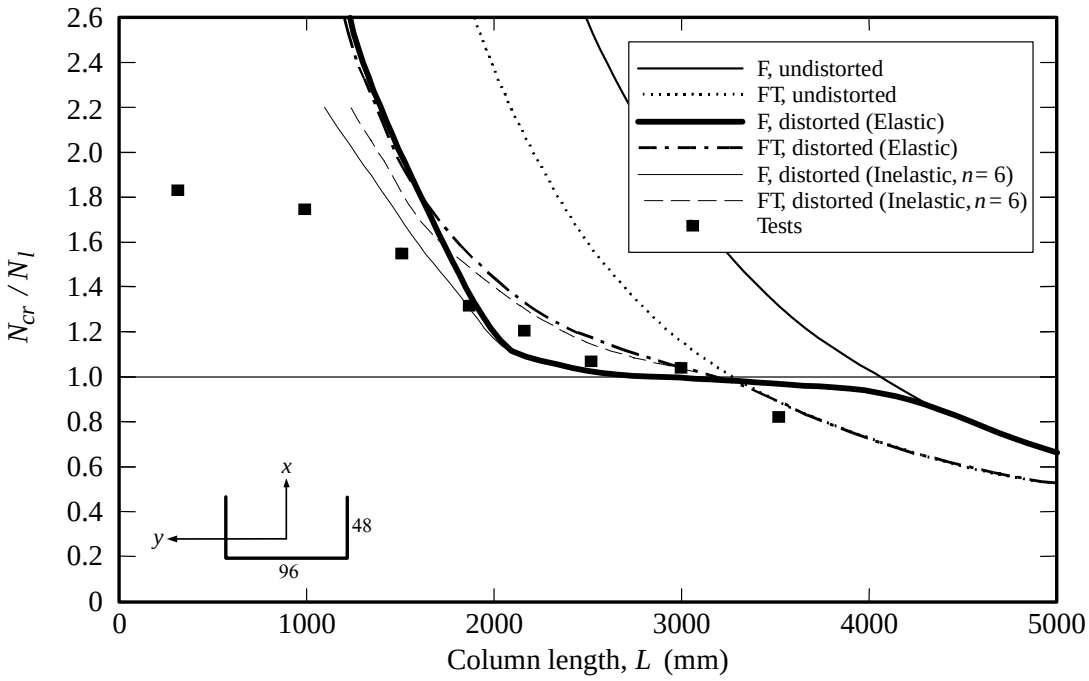

(a) w_o/t = 0.02

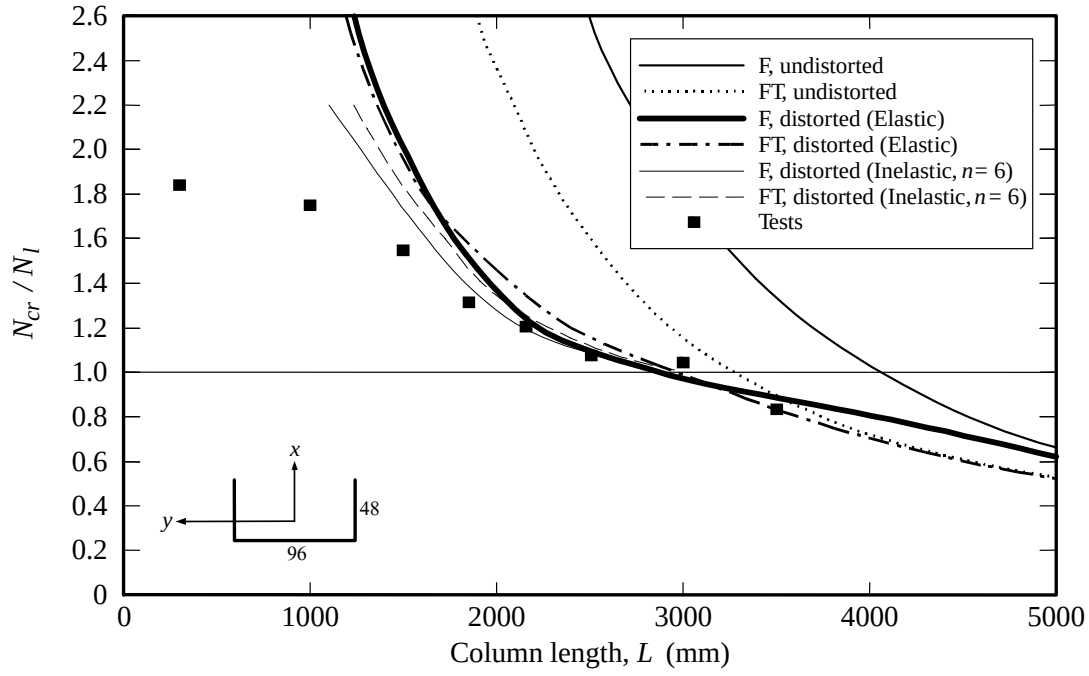

(b) w_o/t = 0.2

Fig. 9. Nondimensionalised load (N_{cr}/N_l) vs column length (L) for fixed-ended P48 channel section

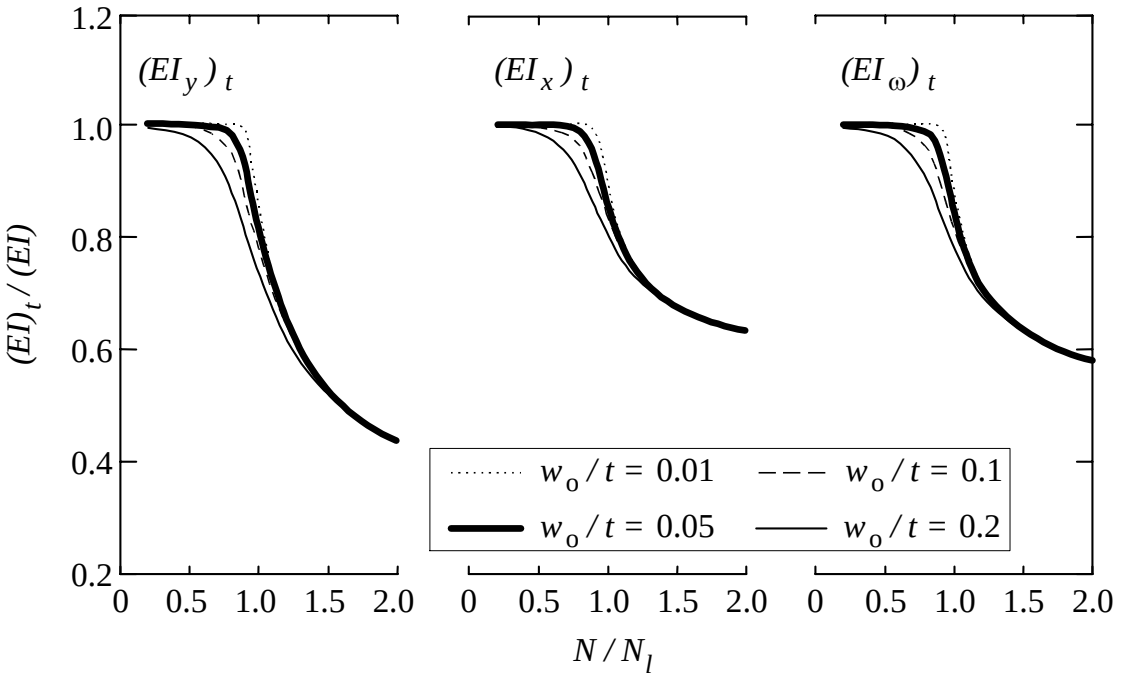

(a) Elastic nonlinear finite strip buckling analysis

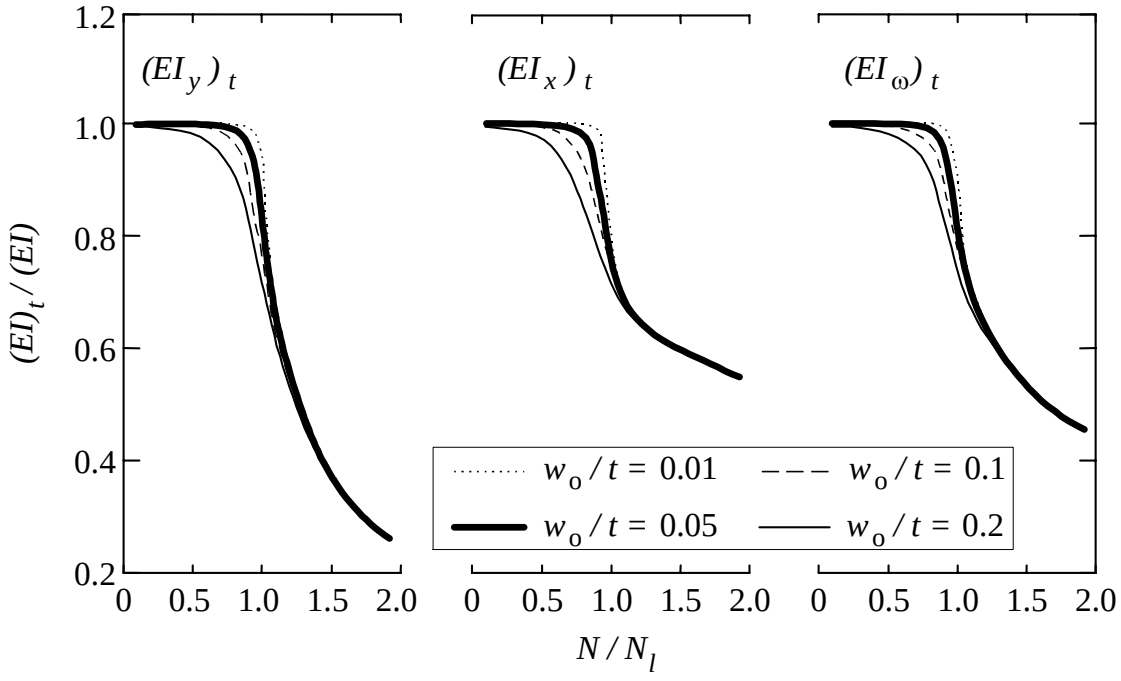

(b) Inelastic nonlinear finite strip buckling analysis

Fig. 10. Tangent rigidity curves for P36 channel section (w_o/t = 0.01, 0.05, 0.1 and 0.2)

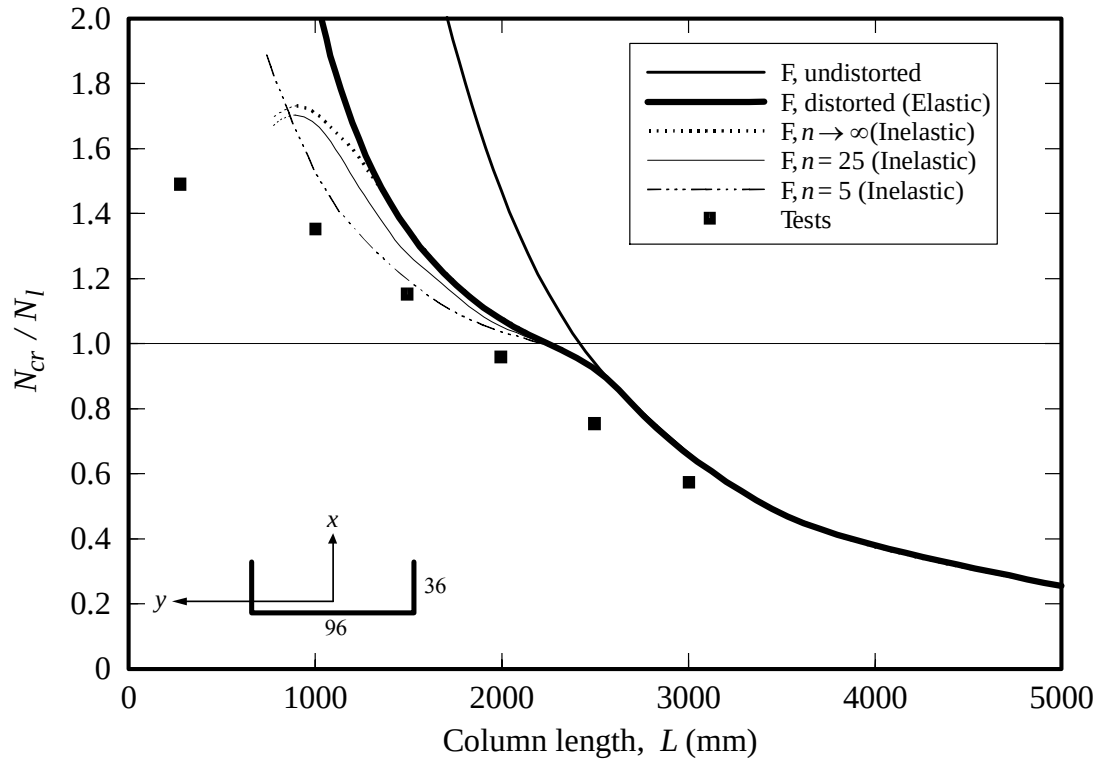

Fig. 11. Flexural inelastic bifurcation curves for P36 channel section (n = 5, 25 and ∞)

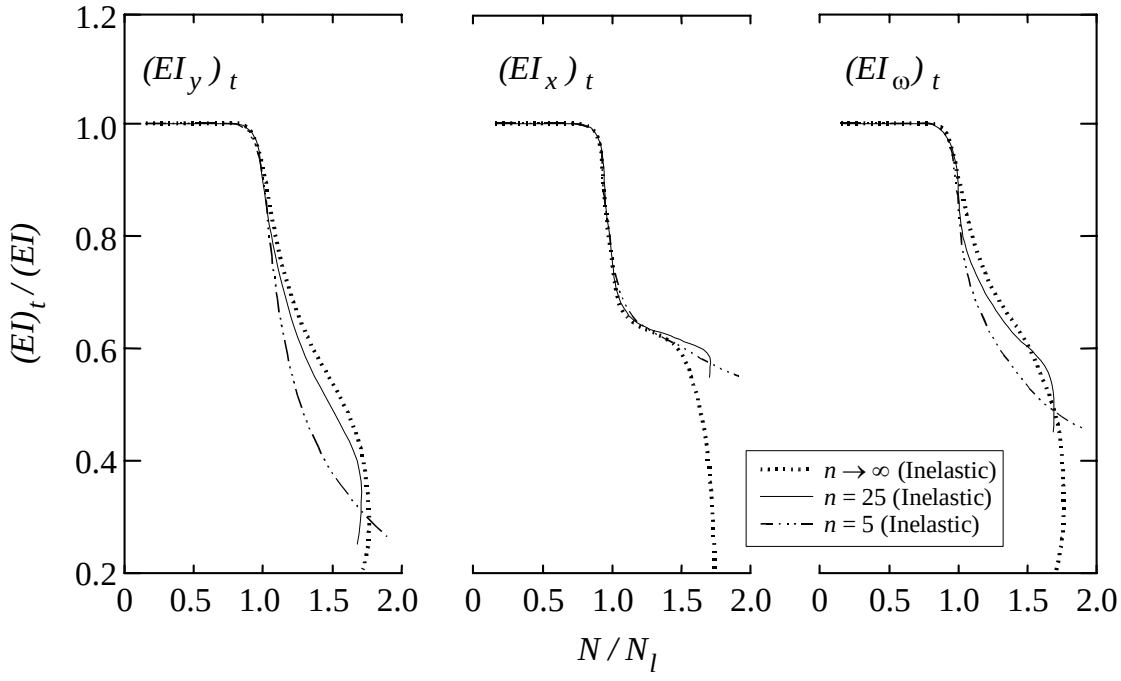

Fig. 12. Inelastic tangent rigidity curves for P36 channel section (n = 5, 25 and ∞)

Tables 1 and 2 are located within the body of the text.

Section	B_f	B_w	t*	r_i	A	I_x	I_y	I_ω	J
	(mm)	(mm)	(mm)	(mm)	(mm^2)	(mm^4)	(mm^4)	(mm^6)	(mm^4)
P36	36.8	96.9	1.47	0.85	247	3.47×10^5	3.10×10^4	4.99×10^7	1.77×10^2
P48	49.6	95.4	1.47	0.85	282	4.17×10^5	7.03×10^4	1.08×10^8	2.03×10^2

* The thickness is the base metal thickness

Table 3. Cross-section dimensions

Series	Local Buckling			Material Properties			
	E	σ_l	l	E_o	$\sigma_{0.01}$	$\sigma_{0.2}$	n
	(MPa)	(MPa)	(mm)	(MPa)	(MPa)	(MPa)	
P36	2.10×10^5	177	110	2.10×10^5	380	550	8
P48	2.10×10^5	128	130	2.10×10^5	320	510	6

Table 4. Local buckling details and measured material properties

APPENDIX A

REFERENCES

Bijlaard, P.P. and Fisher, G.P., (1953). "Column Strength of H-Sections and Square Tubes in Post-buckling range of Component Plates", *National Advisory Committee for Aeronautics,* TN 2994.

Bradford, M.A. and Hancock, G.J., (1984). "Elastic Interaction of Local and Lateral Buckling in Beams", *Thin-walled Structures*, Vol. 2, 1-25.

Davids, A.J. and Hancock, G.J., (1987). "Nonlinear Elastic Response of Locally Buckled Thin-walled Beam-Columns", *Thin-walled Structures,* Vol. 5, 211-226.

Hancock, G.J., (1978). "Local, Distortional and Lateral Buckling of I-Beams", *Journal of the Structural Division,* ASCE, Vol. 104, ST11, 1787-1798.

Hancock, G.J., (1981). "Interaction Buckling in I-Section Columns", *Journal of the Structural Division*, ASCE, Vol. 107, ST1, 165-179.

Hancock, G.J., (1985). "Non-linear Analysis of Thin-walled I-Sections in Bending", *Aspects of Analysis of Plate Structures*, eds D.J. Dawe, R.W. Horsington, A.G. Kamtekar & G.H. Little, 251-268.

Key, P.W. and Hancock, G.J., (1993). "A Finite Strip Method for the Elastic-Plastic Large Displacement Analysis of Thin-walled and Cold-Formed Steel Sections", *Thin-walled Structures*, Vol. 16, 3-29.

Ramberg, W. and Osgood, W.R., (1943). "Description of Stress-Strain curves by Three Parameters", Technical Note No. 902, National Advisory Committee for Aeronautics, Washington, D.C.

Rasmussen, K.J.R., (1995). "Bifurcation Analysis of Locally Buckled Members", *Research Report* R719, School of Civil and Mining Engineering, University of Sydney, *Thin-walled Structures*. (Accepted for publication)

Rasmussen, K.J.R. and Hancock, G.J., (1991). "Nonlinear Analyses of Thin-walled Channel Section Columns", *Thin-walled Structures*, Vol. 13, 145-176.

Rhodes, J. and Harvey, J.M., (1977). "Interaction Behaviour of Plain Channel Columns under Concentric or Eccentric Loading", Proceedings, 2nd International Colloquium on the Stability of Steel Structures, Liege, 439-444.

Young, B. and Rasmussen, K.J.R., (1995a). "Compression Tests of Fixed-ended and Pin-ended Cold-Formed Plain Channels", *Research Report* R714, School of Civil and Mining Engineering, University of Sydney.

APPENDIX B

NOTATION

Latin letters

A	Full cross-section area
B	Bimoment
B_f, B_w	Width of flange, web plate
A, B, C	Constants of quadratic equation
E	Young's modulus
E_o	Initial modulus of elasticity
E_t	Tangential axial stiffness
$(EA)_t$ ... $(GJ)_t$	Tangential rigidities
G	Shear modulus
G_t	Tangential shear stiffness
I_p	Polar moment of area
I_x, I_y	Second moments of area for bending about x, y-axis
I_ω	Warping constant
J	Torsion constant
l	Local buckle half-wavelength
L	Actual column length
M_x, M_y	Bending moment about x, y-axis
n	Cross-sectional coordinate perpendicular to s
n	exponent in Ramberg-Osgood expression
N	Axial force
N_{cr}	Bifurcation buckling load
N_l	Elastic local buckling load
P_x, P_y	Loads for pure flexural buckling about x, y-axis
P_z	Load for pure torsional buckling
q_z	Longitudinal reference stress
r_i	Inside corner radius of specimen
r_o	Polar radius of gyration

s	Cross-sectional coordinate of mid-surface
t	Plate thickness
t^*	Base metal plate thickness
u, v, w, ϕ	Generalised displacements
w_o	Local geometric imperfection (in the shape of the local buckling mode)
W	Wagner stress resultant
x, y	Principal coordinates
x_S, y_S	Coordinates of shear centre
z	Longitudinal coordinate

Greek Letters

ε	Strain
λ	Load factor
λ_c	Load factor at bifurcation
σ	Normal stress
$\sigma_{0.2}$	0.2% proof stress
σ_l	Local buckling stress
ω	Normalised

Conventions

$\delta( )$	Virtual quantity
$(\dot{})$	Infinitesimal increment
$(\bar{})$	Applied action
$( )_o$	Quantity pertains to the fundamental state
$( )_b$	Quantity pertains to the bifurcated state
{ }	Vector
[ ]	Matrix
$\pm, \mp$	Upper and lower of stacked signs are refer to $z = 0$ and $z = L$ respectively.